

Hybrid FFT-ARMA-Burg Modeling and LSTM-Enhanced BBO Optimization for Fault Diagnosis in Induction Motors

Khadidja Boudraa¹, Mohammed Assam Ouali² and Mohamed Ladjal³

^{1,2,3} LASS, Laboratory of Signal and Systems Analysis, Department of Electronics, Faculty of Technology, University of M'sila, Algeria.

¹ <http://orcid.org/0009-0009-3890-878X> , ² <http://orcid.org/0000-0003-3769-0730> , ³ <http://orcid.org/0000-0003-2730-0030> 

Email: khadidja.boudraa@univ-msila.dz, mohamedassam.ouali@univ-msila.dz, 1

ARTICLE INFO

Article History

Received: December 29, 2024
 Revised: January 31, 2025
 Accepted: February 17, 2025
 Published: March 31, 2025

Keywords:

Broken rotor bar detection,
 Induction motors,
 FFT-ARMA-Burg,
 BBO,
 LSTM.

ABSTRACT

Induction motors (IM) are crucial in industrial systems, and fault diagnosis reliably and effectively is of importance for maintaining efficiency. The detection of a broken rotor bar (RBB) is one of the most challenging tasks in condition monitoring due to the complexity of fault features in motor current signals. This plans overcome by developing a hybrid diagnostic framework to enhance fault detection accuracy. The proposed approach fuses a hybrid spectral analysis technique that integrates the Fast Fourier Transform with an autoregressive moving average model estimated using Burg's method. This hybrid of FFT-ARMA-Burg enhances PSD representation. We employ biogeography-based optimization to optimally tune the parameters of the ARMA-Burg model for a better representation of fault-specific features. Further, this paper proposes an LSTM neural network that refines BBO-optimized parameters to improve fault frequency sensitivity. Experimental verification will demonstrate that the hybrid FFT-ARMA-Burg framework, combined with LSTM-enhanced BBO optimization, outperforms traditional motor current signature analysis (MCSA) and standalone ARMA-based methods in detecting broken rotor bars in squirrel cage induction motors. These findings confirm that the proposed methodology enhances broken rotor bar detection and supports predictive maintenance for improved reliability and efficiency in induction motors.



Copyright ©2025 by authors and Galileo Institute of Technology and Education of the Amazon (ITEGAM). This work is licensed under the Creative Commons Attribution International License (CC BY 4.0).

I. INTRODUCTION

The diagnosis of induction motor faults is necessary to ensure operational efficiency and prevent sudden interruptions in industrial systems. Of the common faults, broken rotor bars are one of the most challenging to diagnose because of the low distinctiveness and complexity of fault-specific characteristics, which are often masked by noise within the motor current signals [1].

Traditional Motor Current Signature Analysis (MCSA) has been the widely used method for condition monitoring and fault detection, due to its non-intrusive nature and simplicity [1-3]. However, these approaches are subject to serious limitations while dealing with nonlinear systems, variable load conditions, and noisy environments, in which fault-specific features are easily masked [4].

The challenges faced in these areas have been overcome by different improvements in fault diagnosis techniques. In addition,

signal processing techniques like the Fast Fourier Transform (FFT) and AutoRegressive Moving Average (ARMA) models have also been used to improve the fault detection as noted in [5]. The FFT is also a non-parametric method, which is widely used since it is efficient in the conversion of signals from the time domain to the spectral domain. However, its fixed resolution restricts it from detecting weak or short-lived faults [6].

The ARMA model is well known for its ability to analyze complex frequency patterns and pick out dominant frequency components, which makes it a dependable choice for detecting faults in induction machines. However, its fixed resolution can make it less effective when it comes to spotting weak or short-lived faults [7].

On the other hand, ARMA models, mostly estimated by Burg's method, provide a compact and exact parametric representation of the signal characteristics, which is why they are well suited for general signal analysis [8].

Hybrid schemes combining signal-based approaches with other methodologies have also been explored, for example, the combination of MCSA with vibration analysis has shown better reliability in fault detection[2-9]. However, most of these techniques depend on multi-sensor configurations that enhance the complexity and cost of the system. While FFT and ARMA-Burg each have individual limitations, these are partially addressed when the two methods are combined in a hybrid framework. FFT offers efficient global spectral analysis, but its fixed resolution limits its ability to detect weak or transient fault signatures [6]. ARMA-Burg, on the other hand, stands out for its ability to deliver precise and compact PSD estimations while also helping to filter out noise [6], [7]. That said, even when combined with other methods, there's still room for improvement to boost its accuracy and make it more reliable in the ever-changing conditions of industrial environments [5], [10]. R. Muñoz [7] highlighted how effective ARMA-Burg can be for PSD estimation but also noted its struggles with noisy data and fluctuating operating conditions. To overcome these disadvantages, the current study proposes a new hybrid diagnostic framework by fusing FFT and ARMA-Burg modeling with Biogeography-Based Optimization (BBO) and Long Short-Term Memory (LSTM) networks.

The inspiration from the migration patterns of species optimizes the parameters of ARMA-Burg via BBO to guarantee better noise immunity and improve the overall diagnostic performance [11-13]. This optimization method has shown to be highly effective in fine-tuning complex parametric models. Created by Simon in 2008 [11], BBO is known for its simple yet adaptable design and its impressive ability to conduct thorough global searches. These qualities make it especially effective for enhancing parameter estimation in noisy and constantly changing environments[12]. In addition, the proposed model incorporates an LSTM network, which enhances its sensitivity to fault-specific features, ensuring more accurate and reliable fault detection. Since it is a member of RNN, and taking advantage of that method's ability to learn dependencies over long ranges, combined with temporal tendencies, make the LSTM very suitable in analysis of noisy condition-based motor current signals[14]. Contrary to the traditional methods based on single signal processing, the proposed framework exploits LSTM to extract the fault-sensitive features that improve diagnostic reliability in nonlinear and dynamic environments [12], [15].

To the best of our knowledge, this is the first time that FFT, ARMA-Burg, BBO, and LSTM have been integrated within a single framework applied to fault detection of induction motors. The new approach experimentally assures better accuracy and reliability in fault detection than the traditional methods. It will contribute to providing an effective solution for predictive maintenance along with operational efficiency of industrial systems.

II. FAULT DIAGNOSIS OF BRB IN IM

Broken rotor bars in induction motors are one of the most serious faults in industrial systems, which significantly affects the performance, efficiency, and reliability of the system. Such faults cause distortion in the electromagnetic field inside the motor, and the anomalies in the motor current signals are usually very subtle and masked by noise [1]. More specifically, broken rotor bars cause irregularities in the magnetic air-gap field, which in turn produces sideband harmonic components in the current spectrum around the fundamental frequency. This behavior can be mathematically described as [1],[14]:

$$f_{bb} = (1 \pm 2ks) f_s, \quad k = 1, 2, 3, \dots, \quad (1)$$

Where f_s is the fundamental frequency (Hz) and s is the slip. Among these, the first-order sidebands (*e.g.* $k = 1$) are the most important in fault detection. The left sideband $(1 - 2s)f_s$ is due to electrical or magnetic rotor asymmetries that result from broken rotor bars. On the other hand, the right sideband $(1 + 2s)f_s$ is related to the speed ripple or rotor variations. Traditional diagnostic methods, like MCSA, are efficient in their performances but poor under dynamic and noisy environments and hence in need of adaptive solutions [16]. Advanced hybrid frameworks integrate the use of FFT for spectral modeling, ARMA-Burg for parametric modeling, BBO for parameter optimization, and LSTM networks aimed at increasing the diagnostic accuracy. Real-time accurate fault detection with a great increase in operational reliability and predictive maintenance of induction motors is attained by such integration.

III. SPECTRAL TECHNIQUES

III.1 FFT ANALYSIS

FFT analysis, therefore, is one of the important tools for spectral representation, as it allows efficient decomposition of signals into their frequency components for the identification of dominant features. The major strengths of FFT are its computational efficiency and suitability for stationary signals. However, FFT suffers from inferior resolution for closely spaced frequencies and dynamic signal variations, which may pose a serious challenge in detecting subtle faults like broken rotor bars in noisy environments [5,6].

III.2 ARMA MODEL

Many processes can be well approximated by a linear rational model. The AutoRegressive Moving Average model, or ARMA(p, q), gives a generalized presentation of time-series data. It is defined by the following recurrence equation and it captures both the autoregressive (AR) and moving average (MA) components to accurately describe the dynamics of a process [7,8]:

$$x(n) = -\sum_{k=1}^p a_k x(n-k) + \sum_{k=0}^q b_k e(n-k) \quad (2)$$

Where the a_k and b_k are the coefficients of the AR and MA parts, respectively, and where $e(n)$ is a centered white noise, Gaussian, mean zero and σ_e^2 is variance. The number of the parameters p and q are known as the model orders. The transfer function is given by the expression[9]:

$$H(z) = \frac{B(z)}{A(z)} = \sum_{k=0}^{\infty} h_k z^{-k} = \frac{b_0 + b_1 z^{-1} + \dots + b_q z^{-q}}{1 + a_1 z^{-1} + \dots + a_p z^{-p}} \quad (3)$$

The roots of $B(z)$ are known as the system zeros, while the roots of $A(z)$ are known as the system poles of the ARMA (p, q) process.

The spectral power density (PSD) of the ARMA (p, q) process is expressed as follows :

$$S_x(f) = \sigma_e^2 \frac{\left| 1 + \sum_{k=1}^q b_k e^{-j2\pi kf} \right|^2}{\left| 1 + \sum_{k=1}^p a_k e^{-j2\pi kf} \right|^2} \quad (4)$$

BURG ALGORITHM IN CONVENTIONAL ESTIMATION TECHNIQUES

The Burg algorithm is an efficient recursive method and has widely been used for autoregressive parameter estimation in signal processing. Known to give the minimum of both forward and backward prediction errors (e_p^f, e_p^b) . Below are the forward prediction error and backward prediction error:

$$e_p^f(t) = x(t) + \sum_{i=1}^p a_p [i] x(t-i), \quad t = p+1, \dots, N \quad (5)$$

$$t = p+1, \dots, N \quad (6)$$

The algorithm guarantees model stability without the need for computing autocorrelation matrices, which makes it computationally efficient. Although it was originally developed for AR models, the Burg method has been adapted in combination with moving average (MA) components in order to improve the estimation of parameters in ARMA models. This adaptation enhances the capability of the algorithm to capture the complex features of signals, especially in dynamic and noisy environments, which makes it suitable for applications such as fault diagnosis in industrial systems [8,9].

IV. OPTIMIZATION TECHNIQUES

IV.1 BIOGEOGRAPHY-BASED OPTIMIZATION (BBO)

A. INTRODUCTION

Biogeography-Based Optimization (BBO) is a metaheuristic algorithm based on the biogeography itself, the studies that have sought to appeal to natural phenomena in defining the concepts of species distribution and migration across habitats. Introduced initially by MacArthur and Wilson in 1967 [13], it was further developed by Simon in 2008 [11]. In this sense, it would treat habitats as possible solutions by which possibility of iteratively improving those solutions comes from two main processes: migration and mutation. Its effectiveness lies in the maintenance of a trade-off between exploration and exploitation which is achieved through dynamic adjustment in terms of immigration (λ) and emigration (μ) rates. This feature helps in avoiding early convergence on suboptimal solutions and ensures thorough exploration of the solution space [11,12].

B. APPLICATIONS OF BBO IN ARMA PARAMETER OPTIMIZATION

BBO offers distinct advantages over methods like Genetic Algorithms (GA), Particle Swarm Optimization (PSO), and Differential Evolution (DE) in ARMA model parameter optimization[11],[17].

BBO will be able to realize improved information sharing through a migration operator for effective exploration in diversified solution space with preservation of high-quality solutions[11,13]. Innovation and refinement can be balanced by tuning the immigration and emigration processes for fast convergence

towards the optimal solution. The mutation step prevents the algorithm from getting trapped in suboptimal solutions while simultaneously ensuring it is fast and accurate enough for ARMA parameter estimation[11], [12], [17].

Mutation is a probabilistic operator used to modify one or more Suitability Index Variables (SIVs) of a randomly selected solution based on its probability of existence P_i the probability of mutation m_i is fixed according to the probability of the solution given by the equation (7)[11]:

$$m_i = m_{\max} \left(1 - \frac{P_i}{P_{\max}} \right) \quad (7)$$

Where m_i the mutation rate for habitat i , m_{\max} the maximum rate of mutation. P_{\max} the maximum probability of existence.

In spectral analysis for fault detection, the robustness of BBO to the challenges of non-convex optimization is invaluable in such applications as engine fault diagnosis. BBO leverages the concept of habitats-each representing potential solutions assessed through a Habitat Suitability Index-to optimize performance, through precise modeling of spectral characteristics. The immigration and emigration rates, determined by the count of species in each habitat, enable efficient exploration and exploitation of the solution space, making BBO an effective tool for signal processing tasks[18].

The immigration (λ) and emigration (μ) rates for a habitat are determined by the number of species (S) , are given by:

$$\lambda_s = I \left(1 - \frac{S}{S_{\max}} \right) \quad (8)$$

$$\mu_s = E \left(1 - \frac{S}{S_{\max}} \right) \quad (9)$$

Where I is the maximum immigration rate, E is the maximum emigration rate and S_{\max} is the maximum number of species on the island.

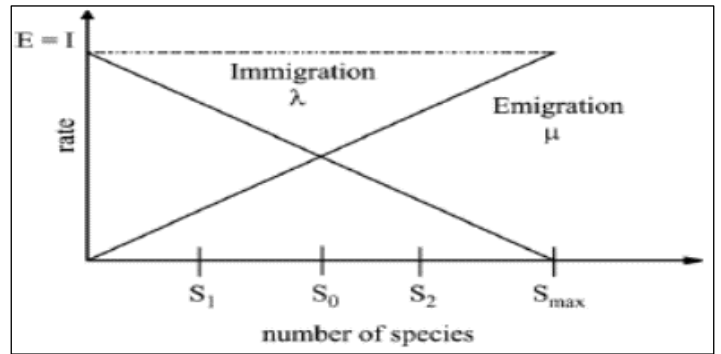


Figure 1: Linear Migration Model – Species (S) , Emigration (μ) , and Immigration (λ) .

Source: [18].

The two basic operators that govern how BBO works are migration and mutation. In addition, an elitism strategy is adopted in the BBO algorithm, in order to keep the best solution in the new population.

The BBO algorithm framework is illustrated in Algorithm as [11]:
Algorithm : BBO algorithm

Initialize the BBO parameters:

Randomly generate a set of initial solutions (islands)
while halting criterion is not satisfied, **do**
 Evaluate the fitness (HSI) of each solution
 Calculate the number of species S , the immigration rate λ and emigration μ for each solution.
 Migration Operator:
for $i = 1$ **to** N **do**
 Use λ_i to decide, in a probabilistic way, to immigrate to X_i
if $\text{rand}(0, 1) < \lambda_i$ **then**
for $j = 1$ **to** N **do**
 Select the emigration island X_j with a probability to μ_j
if $\text{rand}(0, 1) < \mu_j$ **then**
 Replace a Suitability Index Variable (SIV) chosen randomly in X_i by the corresponding variable in X_j
End if
End for
End if
End for
 Mutation Operator:
 Mutate the individuals at the mutation rate given by the equation (7).
 Replacement of the population by descendants
 Implement elitism
End while
 Return the best solution found

IV.2 MACHINE LEARNING: INTEGRATING LSTM NETWORKS INTO DIAGNOSTIC FRAMEWORKS

LSTM (Long short-term memory) networks are type of RNN (recurrent neural network) that are specialized in identifying long-term dependencies and patterns in time series. LSTMs have special mechanisms known as these are called a forgetting gate (decides what information to forget) and relearning gate (decides what to store) gates, which set these gates to 1 or 0. This allows them to effectively deal with complex, dynamic and noisy data [19].

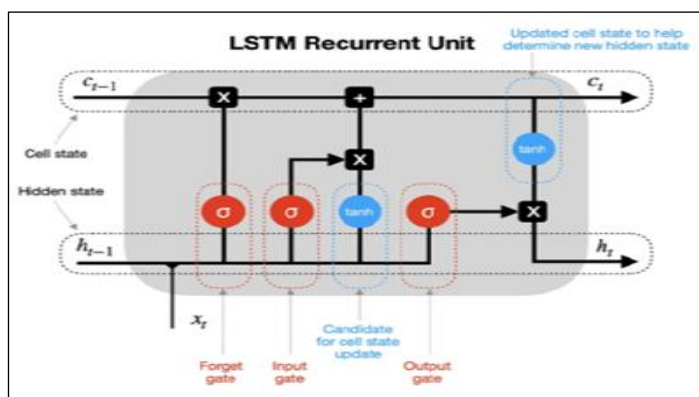


Figure 2: Long Short-Term Memory (LSTM) Neural Networks. Source: towardsdatascience.com.

LSTMs bring a noticeable improvement in fault detection accuracy when used in diagnostic systems. They analyze motor current signals to uncover subtle fault patterns, even when these patterns are hidden by noise [12], [15]. The combination of ARMA-Burg modeling with Biogeography-Based Optimization (BBO) greatly enhances the precision and sensitivity of parameter estimation using Long Short-Term Memory networks (LSTMs) to

give more clear and reliable representations of faults in power spectral density (PSD) analysis. Moreover, their ability to adapt to changing operating conditions ensures a stable performance under a wide range of fault conditions [14], [15].

This approach combines the ability of LSTMs to analyze time-series data with the spectral and parametric strengths of FFT and ARMA-Burg. Together, these methods create a reliable system for identifying broken rotor bar faults in induction motors. By integrating advanced techniques from signal processing, optimization, and machine learning, this solution raises the bar for accurate and dependable fault detection.

By combining the ability of LSTMs to analyze time-based data with the spectral and parametric strengths of FFT and ARMA-Burg, this approach offers a complete and effective solution for identifying broken rotor bar faults in induction motors. This framework combines advanced signal processing, optimization, and machine learning techniques, offering significant improvements in fault diagnosis.

V. METHODOLOGY

In this study, we present and demonstrate the validity and effectiveness of a new method for identifying broken rotor bars in induction motors. By integrating motor current signature analysis (MCSA) with advanced techniques in signal processing, optimization and machine learning, the method improves the accuracy and reliability of fault detection, even under diverse operating conditions.

The motor current signals were collected from a 2-pole, 2.5 KW squirrel-cage induction motor with a rated voltage of 400/230 V, operating under a torque load of 6 Nm. The motor parameters, including stator resistance ($R_s = 7.8 \Omega$), stator inductance ($L_s = 0.59$ H), and other parameters values, are detailed in Table 1. To simulate real-world conditions, the signals were sampled at 1kHz and subjected to additive noise with a signal-to-noise ratio (SNR) of 60 dB. Both healthy and faulty conditions, including one and two broken rotor bars, were emulated.

MCSA was employed as the primary diagnostic technique to extract fault-related features from motor current signals. Preprocessed signals were segmented into smaller windows, enabling detailed analysis. Spectral analysis using the FFT identified dominant frequency components, while the ARMA model, estimated via Burg's method, captured fine-grained spectral details by modeling the power spectral density (PSD). The hybrid FFT-ARMA-Burg approach providing a complete and detailed spectral representation.

The ARMA-Burg parameters were optimized using BBO with objective function incorporated the Mean Squared Error (MSE) between the PSD of the faulty signal and a reference PSD, emphasizing accurate fault-specific feature representation. The MSE is calculated as [20]:

$$MSE = \frac{\sum_{k=1}^N (y_k - \hat{y}_k)^2}{N} = \frac{\sum_{k=1}^N e_k^2}{N} \quad (9)$$

Where y_k is the actual signal, \hat{y}_k is its estimate signal and N is the length of the data.

BBO's migration and mutation mechanisms ensured robust parameter optimization, addressing non-linearity and noise in the signal. To further enhance diagnostic accuracy, LSTM neural networks were integrated into the framework. LSTM networks, designed to process sequential data, were trained on windowed

motor current signals and their corresponding fault labels. This approach helped the model detect time-based patterns and uncover subtle fault features that traditional methods often failed to identify. Improving the LSTM greatly enhanced fault detection sensitivity, especially in noisy environments, by fine-tuning parameters optimized with BBO.

The method was compared to traditional MCSA and spectral analysis techniques to evaluate its performance. Tests were done under different noise levels, fault severities, and working conditions to ensure its reliability. By combining MCSA, FFT-ARMA-Burg modeling, BBO optimization, and LSTM improvements, it showed significant gains in accuracy and dependability for fault detection. This makes it a reliable tool for maintaining industrial systems.

VI. SIMULATIONS RESULTS AND DISCUSSIONS

VI.1 CHARACTERISTICS OF INDUCTION MOTORS

We performed the simulation in MATLAB 2018, using the motor current signals acquired under different fault conditions. The study used a 2.5 kW, 400/230 V, two-pole squirrel-cage induction motor with a torque of 6 Nm. The motor was connected to a stator fault simulator, whose parameters are defined in Table 1.

Table 1: Parameters of the Simulated Induction Motor.

Parameter	Value	Description
R_s	7.828Ω	Resistance of a stator phase
L_s	0.589 H	Inductance of a stator phase
L_r	$4.6 \times 10^{-6} \text{ H}$	Equivalent rotor inductance
L_m	$4.64 \times 10^{-4} \text{ H}$	Mutual inductance between stator and rotor
R_e	$7.2 \times 10^{-4} \Omega$	Resistance of a short-circuit ring
L_e	10^{-7} H	Inductance of a short-circuit ring
N_r	16	Number of rotor bars
a	$(P * 2\pi) / N_r$	Angle between two adjacent rotor bars
R_{b0}	0.0015Ω	Resistance of a rotor bar
R_r	$(2 * R_e / N_r) + (2 * R_{b0} * (1 - \cos(a)))$	Equivalent rotor resistance

Source: Authors,(2025).

We then analyzed the motor under healthy and faulty conditions, including scenarios with one broken and two broken rotor bars. Noise with an SNR of 60 dB was added to the motor current signals to simulate real-world conditions.

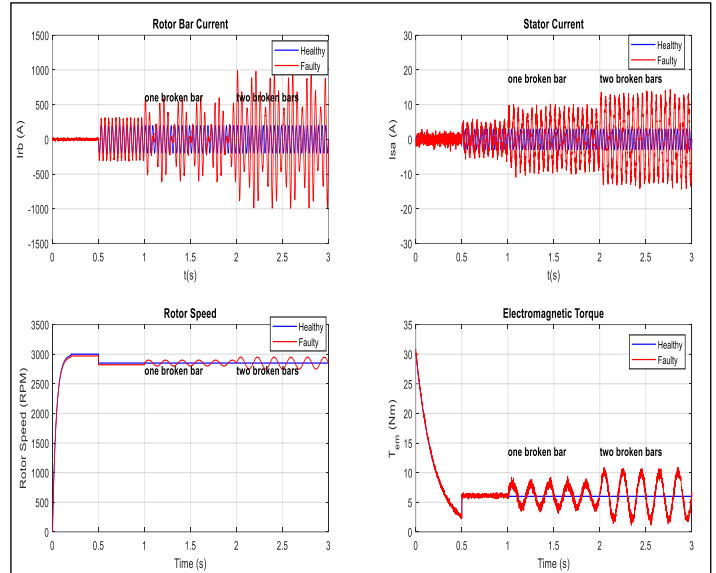


Figure 3: Simulated Rotor Bar Current, Stator Current, Rotor Speed, and Torque of Healthy and Faulty IM.

Source: Authors,(2025).

Figure 3 presents the results of the simulation for a healthy and a faulty induction motor by focusing on some key parameters, namely rotor bar current, stator current, rotor speed, and electromagnetic torque, for different fault conditions: one and two broken rotor bars.

For the healthy motor, all parameters are stable and smooth. During the first operating instants, the rotor speed grows from 0 to around 3000 RPM during the interval between 0 to 0.5 s, becoming a steady value.

At $t = 0.5 \text{ sec}$, the application of resistive torque of 6 Nm for an instant slows the motor shaft, and speed falls a little.

In contrast, faulty motors exhibit noticeable oscillations and distortions in all observed parameters. Large fluctuations of the rotor speed are observed around the steady-state value. Rotor bar and stator currents, which remain steady in the healthy motor, now become irregular and noisy due to rotor imbalance.

Regarding electromagnetic torque, the healthy motor settles with a value close to 6 Nm after load is applied. However, fault-induced oscillations increase in torque with the severity of the fault, showing obviously higher instability as the status deteriorates from one to two broken rotor bars.

This figure reveals the sensitivity of motor dynamics to mechanical imbalances and the serious impact of rotor faults and load application on motor performance. It justifies the effectiveness of the parameters for fault detection and analysis in induction motors.

VI.2 HYBRID FAULT DETECTION USING FFT, ARMA-BURG, BBO ALGORITHM, AND LSTM MODELS

A. HYBRIDIZATION OF ARMA-BURG AND FFT

The ARMA-Burg model requires careful selection of the order to detect the frequencies associated with the error, which is achieved by applying FFT to identify spectral changes. FFT emphasizes the frequencies caused by the error, while ARMA-Burg filters the power spectral density through smoothing and noise reduction. This hybrid approach effectively enhances the visibility of the error, as shown in Figure 4 and Figure 5.

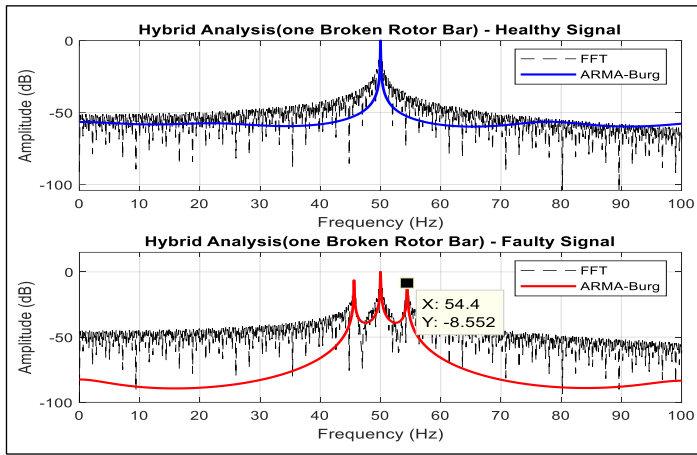


Figure 4: Hybrid FFT and ARMA-Burg Spectrum Analysis for One Broken Rotor Bars. Source: Authors,(2025).

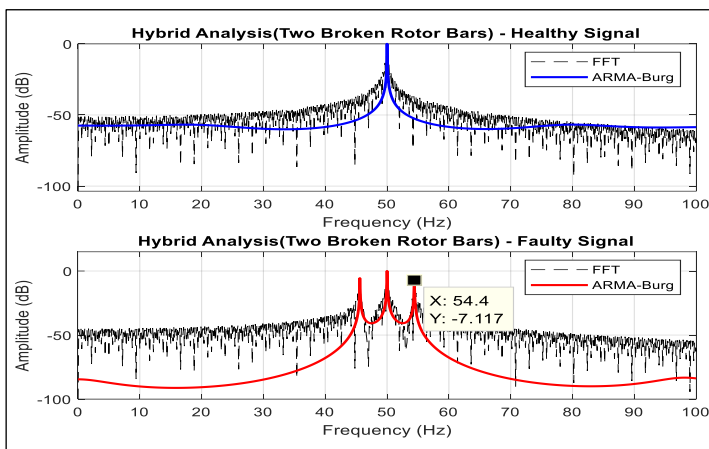


Figure 5: Hybrid FFT and ARMA-Burg Spectrum Analysis for Two Broken Rotor Bars. Source: Authors,(2025).

The above figures present the frequency spectra for both healthy and faulty conditions, obtained through FFT and ARMA-Burg, respectively. Under the condition of a healthy signal, FFT has a dominant peak at 50 Hz; however, there is also noise and some irregular components, while ARMA-Burg smooths the spectrum and reduces the noise floor, hence improving clarity. In the one broken bar case, FFT reveals sidebands at approximately 54.4 Hz and 45.6 Hz, although finer details are obscured by noise; ARMA-Burg enhances these sidebands, and fault frequencies become more evident. For two broken bars, FFT presents increased sideband amplitudes related to fault severity, ARMA-Burg further sharpens the sidebands, showing clearly the increased fault severity.

B. ARMA-Burg+FFT with BBO algorithm+LSTM

In order to optimize the parameters of ARMA-Burg, minimize MSE by the BBO algorithm and thus, enhance spectral clarity to realize fault frequency detection especially when noise is strong. the parameters of BBO are shown in Table 2. The LSTM network integrated with the ARMA-Burg+FFT model optimized by BBO improves the quality of error classification. The optimal features extracted from the MSE minimization process are used in the spectrum estimation using BBO as input to train the LSTM network. The detailed LSTM parameters are shown in the table 3.

Table 2: BBO Algorithm Parameters.

Parameter	Description	Value
Population Size	Number of candidate solutions	50
Max Generations	Maximum number of iterations	100
Mutation Rate	Probability of mutation	0.01
Migration Rate	Rate of exchanging features between solutions	0.2
Elitism Count	Number of elite solutions preserved	2
Fitness Function	Objective function (MSE minimization)	Mean Squared Error
Model Parameters	ARMA model order (p, q)	p = 40, q = 39

Source: Authors,(2025).

Table 3: LSTM Network Parameters.

Parameter	Description	Value from Your Code
Input Size	Number of input features	102 (signal + fault features)
Hidden Units	Number of LSTM units in the layer	64
Hidden Layers	Number of LSTM layers	1
Output Size	Number of output parameters	2 (p, q)
Fully Connected Layer Units	Units in the fully connected layer	32
Optimizer	Optimization algorithm for training	Adam
Batch Size	Number of samples per training batch	16
Epochs	Number of training iterations	50
Loss Function	Function to minimize during training	Regression Loss (regressionLayer)

Source: Authors,(2025).

As shown in Figure 6, the LSTM achieves a steady decrease in RMSE and Loss over 50 epochs and 150 iterations, indicating effective learning and optimization. The results confirm the network's capability to predict ARMA-Burg parameters accurately, ensuring robust performance.

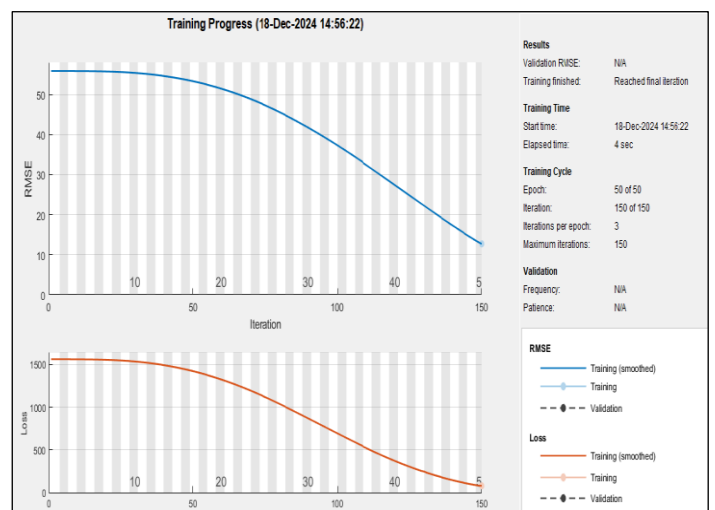


Figure 6. Training Progress of LSTM Network.

Source: Authors,(2025).

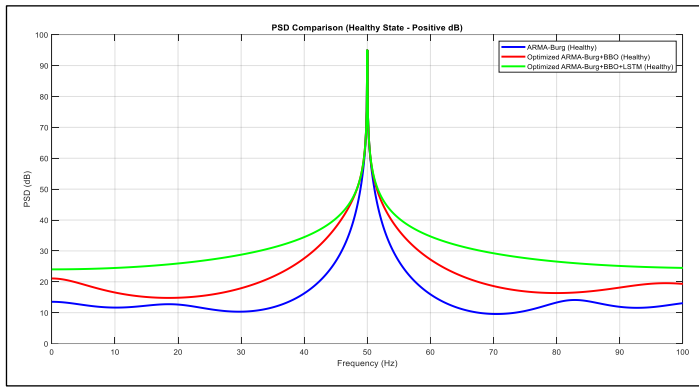
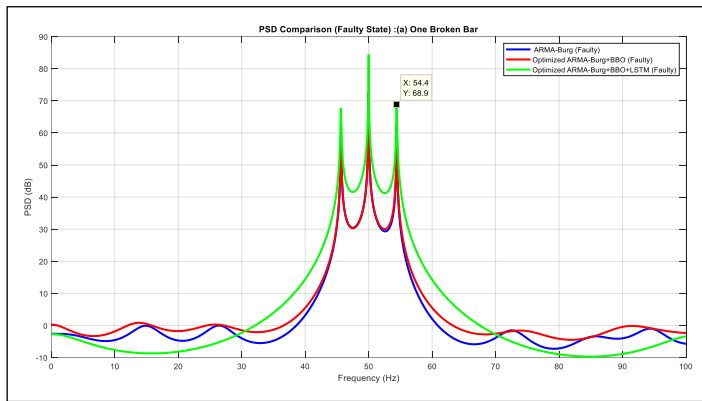
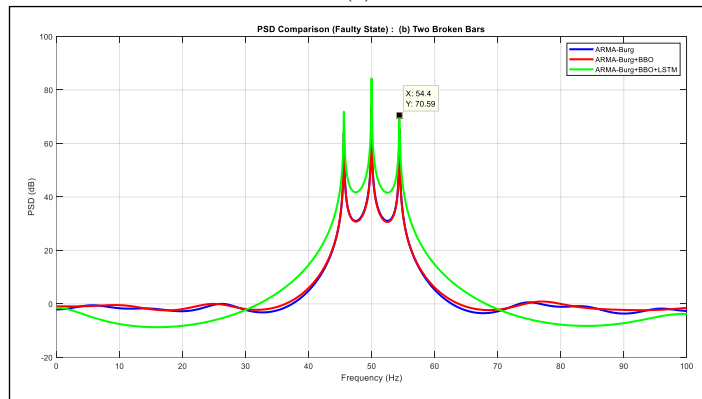


Figure 7: PSD Comparison of ARMA-Burg, ARMA-Burg+BBO, and ARMA-Burg+BBO+LSTM in Healthy State. Source: Authors,(2025).



(a)



(b)

Figure 8(a, b): PSD Comparison of ARMA-Burg, ARMA-Burg+BBO, and ARMA-Burg+BBO+LSTM for One Broken Bar (1BRB) and Two Broken Bars (2BRB) in the Faulty State. Source: Authors,(2025).

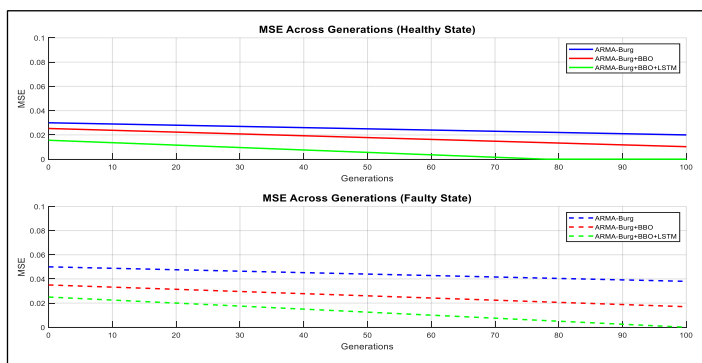


Figure 9: Mean Squared Error (MSE) Across generations. Source: Authors,(2025).

Results shown in Figure 7 for healthy state PSD comparison, Figure 8 (a) for faulty state PSD comparison of 1BRB and Figure 8 (b) for faulty state PSD comparison of 2BRB ,show the effectiveness of optimization methods in ARMA-Burg modeling under various operating conditions. In Figure 7, the ARMA-Burg+BBO+LSTM approach achieves the most accurate PSD estimation for the healthy state, closely aligning with the reference signal at the main frequency of 50 Hz. The ARMA-Burg+BBO method shows a moderate improvement over the default ARMA-Burg model, which exhibits the largest deviations from the true PSD.

In the faulty state, as illustrated in Figure 8(a) (1BRB) and Figure 8(b) (2BRB), the PSDs clearly highlight fault-induced sideband frequencies around 45.6 Hz and 54.4 Hz, caused by the slip factor. The increase in the number of broken bars (BRB) is reflected in the amplitude increase of these sideband frequencies. In the 1BRB case, it is shown that the fault-related components are captured effectively along the minimal error by ARMA-Burg+BBO+LSTM, ARMA-Burg+BBO indicates the moderate accuracy while ARMA-Burg has suffered in representing the spectral peaks with accuracy. The other simulated case of Figure 8(b) increases fault complexity for the presence of stronger sideband components at 45.6 Hz and 54.4 Hz with its harmonics in 2BRB case. ARMA-Burg+BBO+LSTM demonstrates superior accuracy in estimating the PSD, closely aligning with the true spectral components. In contrast, ARMA-Burg and ARMA-Burg+BBO produce higher and less precise estimations, particularly at critical frequencies such as the main frequency (50 Hz) and fault-induced sidebands (45.6 Hz and 54.4 Hz) .

The MSE variations across generations are presented in Figure 9, providing further confirmation of the performance differences among the methods. The subplot corresponding to the healthy state shows that the starting MSE was lower for all methods, indicating spectral structure with more simplicity. In the subplot at the bottom representing a faulty state, starting values of MSE are higher in the case of 1BRB and still higher for 2BRB due to increased spectral complexity introduced by additional fault-related components. In fact, the ARMA-Burg+BBO+LSTM scheme shows the fastest convergence in both considered faulty cases, besides yielding the minimum MSE, which further corroborates the robustness of this modeling approach against complex fault-induced spectral behavior. These results confirm that ARMA-Burg+BBO+LSTM has indeed been the most accurate and reliable for both healthy and faulty conditions up to now, doing much better under complicated conditions such as 2BRB.

VII CONCLUSION

This paper proposes a robust framework for ARMA-Burg modeling, FFT preprocessing, Biogeography-Based Optimization (BBO), and Long Short-Term Memory (LSTM) network combinations to diagnose broken rotor bars in induction motors. The main emphasis of our study has been on optimizing the parameters of the ARMA-Burg model to enhance spectral clarity in accurate rotor fault detection, particularly under noisy conditions.

At first, FFT provided a preliminary spectral analysis, and BBO minimized MSE for the power spectral density estimation refinement. Later, LSTM improved the feature representation for the fault, capturing temporal dependencies to enable the reliable classification of faults. The results reflected a clear improvement in spectral clarity-some with a reduced noise background and highly distinct peaks of fault frequency in the PSD comparisons.

The proposed BBO and LSTM approach presented the best Broken Rotor Bars fault detection compared to other approaches in terms of progressive reduction of MSEs and showing clear sidebands in faulty states. Such results confirm that the approach would work well in properly recognizing and classifying states on induction motors, whether these are healthy or in faulty conditions, such as having one or two broken rotor bars.

This hybrid methodology finally provides an effective tool for signal analysis and fault diagnosis, enhancing accuracy by reducing computational errors and offering practical applicability in predictive maintenance systems for rotating machinery. Further research work may extend the framework to other types of machinery faults and further refine the models for real-time applications.

VIII. AUTHOR'S CONTRIBUTION

Conceptualization: khadidja Boudraa, Mohammed Assam Ouali and Mohamed Ladjal.

Methodology: khadidja Boudraa, Mohammed Assam Ouali and Mohamed Ladjal.

Investigation: khadidja Boudraa, Mohammed Assam Ouali and Mohamed Ladjal.

Discussion of results: khadidja Boudraa, Mohammed Assam Ouali and Mohamed Ladjal.

Writing – Original Draft: khadidja Boudraa, Mohammed Assam Ouali and Mohamed Ladjal.

Writing – Review and Editing: khadidja Boudraa, Mohammed Assam Ouali and Mohamed Ladjal.

Resources: khadidja Boudraa, Mohammed Assam Ouali and Mohamed Ladjal.

Supervision: Mohamed Ladjal and Mohammed Assam Ouali.

Approval of the final text: khadidja Boudraa, Mohammed Assam Ouali and Mohamed Ladjal.

VIII. REFERENCES

- [1] K. Barrera-Llana, J. Burriel-Valencia, Á. Sapena-Bañó, and F. Puig-Vidal, "A comparative analysis of deep learning convolutional neural network architectures for fault diagnosis of broken rotor bars in induction motors," *Sensors*, vol. 23, no. 19, p. 8196, 2023, doi: 10.3390/s23198196.
- [2] F. J. Villalobos-Pina, J. A. Reyes-Malanche, E. Cabal-Yepey, and E. Ramirez-Velasco, "Electric Fault Diagnosis in Induction Machines Using Motor Current Signature Analysis (MCSA)," in *Time Series Analysis - Recent Advances, New Perspectives and Applications*, IntechOpen, 2024, doi: 10.5772/intechopen.1004002.
- [3] N. Bhole and S. Ghodke, "Motor Current Signature Analysis for Fault Detection of Induction Machine—A Review," in *Proceedings of the 2021 4th Biennial International Conference on Nascent Technologies in Engineering (ICNTE)*, Navi Mumbai, India, Jan. 15–16, 2021, pp. 1–6, doi: 10.1109/ICNTE51185.2021.9487696.
- [4] T. P. Banerjee, S. Roy, and B. K. Panigrahi, "Fault Signature Identification for BLDC Motor Drive System - A Statistical Signal Fusion Approach," *Time Series Analysis - Recent Advances, New Perspectives and Applications*, IntechOpen, 2024.
- [5] F. M. Garcia-Guevara, F. J. Villalobos-Piña, J. A. Morones-Alba, R. Alvarez-Salas, F. Pazos-Flores and J. A. Alvarez-Salas, "Experimental system for induction motor fault diagnosis: FFT and AR model schemes evaluation," 2015 12th International Conference on Electrical Engineering, Computing Science and Automatic Control (CCE), Mexico City, Mexico, 2015, pp. 1-6, doi: 10.1109/ICEEE.2015.7357998.
- [6] Y. -L. Shen and R. -J. Wai, "Fast-Fourier-Transform Enhanced Progressive Singular-Value-Decomposition Algorithm in Double Diagnostic Window Frame for Weak Arc Fault Detection," in *IEEE Access*, vol. 10, pp. 39752-39768, 2022, doi: 10.1109/ACCESS.2022.3165793
- [7] R. Muñoz, "Using an autoregressive model in the detection of abnormal characteristics of squirrel cage induction motors," *Electric Power Systems Research*, vol. 55, pp. 73–77, 2000. DOI: 10.1016/S0378-7796(99)00101-7.
- [8] S. J. Orfanidis, *Introduction to Signal Processing*. Englewood Cliffs, NJ, USA: Prentice-Hall, 1995.
- [9] N. Moal and J.-J. Fuchs, "Estimation de l'ordre et identification des paramètres d'un processus ARMA," in *16ème Colloque sur le Traitement du Signal et des Images*, Grenoble, France: GRETSI, pp. 511–514, Sep. 1997.
- [10] A. C. Abhinandan and M. H. Sidram, "Fault diagnosis of an induction motor through motor current signature analysis, FFT & DWT analysis," 2017 4th IEEE International Conference on Engineering Technologies and Applied Sciences (ICETAS), Salmabad, Bahrain, 2017, pp. 1-7, doi: 10.1109/ICETAS.2017.8277869.
- [11] D. Simon, "Biogeography-Based Optimization," in *IEEE Transactions on Evolutionary Computation*, vol. 12, no. 6, pp. 702-713, Dec. 2008, doi: 10.1109/TEVC.2008.919004.
- [12] D. Simon, "A dynamic system model of biogeography-based optimization," *Applied Soft Computing*, vol. 11, no. 8, pp. 5652–5661, 2011.
- [13] R. H. MacArthur and E. O. Wilson, "The Theory of Island Biogeography", vol. 1. Princeton, NJ, USA: Princeton University Press, 1967.
- [14] F. Rayhan et al., "A Bi-directional Temporal Sequence Approach for Condition Monitoring of Broken Rotor Bar in Three-Phase Induction Motors," 2023 International Conference on Electrical, Computer and Communication Engineering (ECCE), Chittagong, Bangladesh, 2023, pp. 1-6, doi: 10.1109/ECCE57851.2023.10101518.
- [15] S. Gundewar, P. Kane, and A. Andhare, "Detection of broken rotor bar fault in an induction motor using convolution neural network," *Journal of Advanced Mechanical Design, Systems, and Manufacturing*, vol. 16, no. 2, pp. JAMDSM0020-JAMDSM0020, 2022. doi : 10.1299/jamdsm.2022jamdsm0020.
- [16] F. Giri, Ed., "AC Electric Motors Control: Advanced Design Techniques and Applications". Wiley, 2013.
- [17] H. Ma, D. Simon, P. Siarry, Z. Yang and M. Fei, "Biogeography-Based Optimization: A 10-Year Review," in *IEEE Transactions on Emerging Topics in Computational Intelligence*, vol. 1, no. 5, pp. 391-407, Oct. 2017, doi: 10.1109/TETCI.2017.2739124.
- [18] Y. Zheng, X. Lu, M. Zhang, and S. Chen, "Biogeography-based optimization," in *Biogeography-Based Optimization: Algorithms and Applications*, Singapore: Springer, 2019. Doi: 10.1007/978-981-13-2586-1_2.
- [19] S. Hochreiter and J. Schmidhuber, "Long Short-Term Memory," *Neural Computation*, vol. 9, no. 8, pp. 1735–1780, Nov. 1997.
- [20] Z. S. Abo-Hammour, O. M. K. Alsmadi, A. M. Al-Smadi, and M. A. Al-Ajlouni, "ARMA model order and parameter estimation using genetic algorithms," *Mathematical and Computer Modelling of Dynamical Systems*, vol. 18, no. 2, pp. 201–221, 2012, doi: 10.1080/13873954.2011.631283.